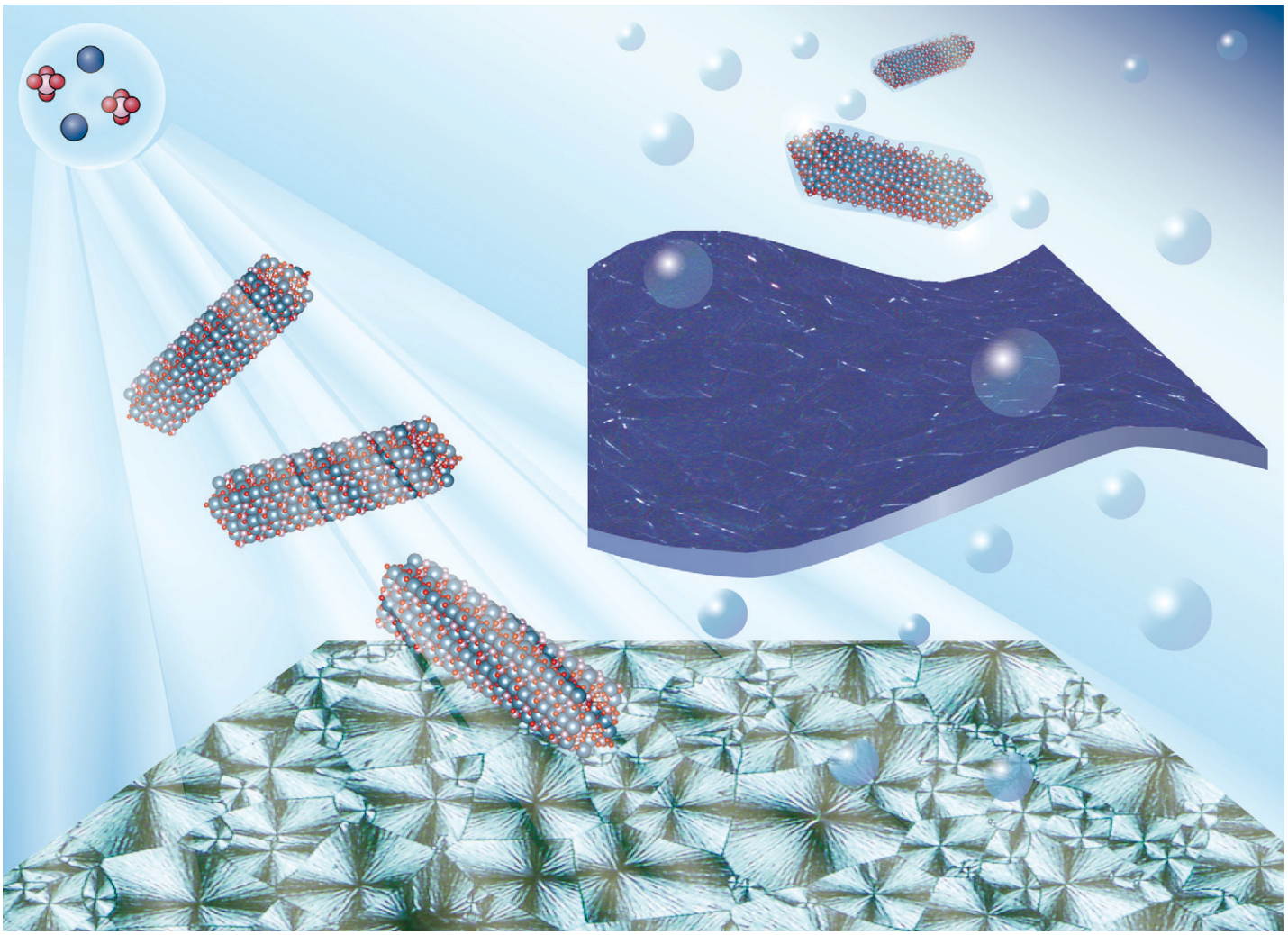

Showcasing collaborative research by Satoshi Kajiyama, Takeshi Sakamoto, Moe Inoue, Tatsuya Nishimura, Taishi Yokoi, Chikara Ohtsuki and Takashi Kato* from Department of Chemistry and Biotechnology, School of Engineering, the University of Tokyo, Japan.

Rapid and topotactic transformation from octacalcium phosphate to hydroxyapatite (HAP): a new approach to self-organization of free-standing thin-film HAP-based nanohybrids

Free-standing hydroxyapatite hybrid thin films with submicrometer thickness are obtained from self-organized hybrid films of octacalcium phosphate through the rapid and topotactic transformation in aqueous media.

As featured in:

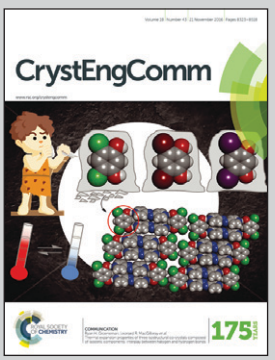

See Takashi Kato *et al.*, *CrystEngComm*, 2016, **18**, 8388.

ROYAL SOCIETY OF CHEMISTRY

www.rsc.org/crystengcomm

Registered charity number: 207890

CrystEngComm

PAPER

View Article Online
View Journal | View Issue

Cite this: *CrystEngComm*, 2016, **18**, 8388

Rapid and topotactic transformation from octacalcium phosphate to hydroxyapatite (HAP): a new approach to self-organization of free-standing thin-film HAP-based nanohybrids†

Satoshi Kajiyama,[a] Takeshi Sakamoto,[a] Moe Inoue,[a] Tatsuya Nishimura,‡[a] Taishi Yokoi,[b] Chikara Ohtsuki[b] and Takashi Kato*[a]

Received 10th June 2016,
Accepted 30th September 2016

DOI: 10.1039/c6ce01336h

www.rsc.org/crystengcomm

Biomineralization-inspired processing is attractive for the preparation of functionalized inorganic/organic polymer hybrid materials because the materials are obtained under mild conditions and by using organic templates. As for the formation processes of ordered nanocrystalline hydroxyapatite (HAP), the preparation of self-standing hybrid films based on HAP has not yet been established. In the present study, self-standing thin-film hybrids composed of HAP and poly(vinyl alcohol) (PVA) are obtained by rapid and topotactic transformation of thin films based on octacalcium phosphate (OCP) as a precursor in the organic polymer matrix. Bioinspired crystallization of calcium phosphate on the PVA matrix in the presence of poly(acrylic acid) leads to the formation of nanocomposite structures with oriented OCP nanorod crystals 2–4 nm in width and 10–30 nm in length. The nanostructures allow the composites to transform rapidly into a HAP/PVA hybrid thin film in water. The transformation proceeds without a change in the original OCP/PVA nanostructures, resulting in the formation of a HAP/PVA hybrid thin film with oriented HAP nanorod crystals 5–6 nm in width and 20–50 nm in length. The HAP/PVA hybrids have been obtained as self-standing films with submicrometer scale thickness. The ratio of organic to inorganic components in the self-standing hybrid thin films is similar to that in bones of vertebrates.

Introduction

Biominerals have attracted increasing attention because of their hierarchical functional composite structures from the nano- to macro-scale.[1] It is noteworthy that they are formed under mild conditions.[2,3] For example, teeth have nano-scale ordered structures consisting of hydroxyapatite (HAP; $Ca_{10}(PO_4)_6(OH)_2$) nanorod crystals, which exhibit high compressive strengths.[3] HAP is now recognized as an important functional material. If thin films composed of HAP crystals are formed under mild conditions, new, stable and biocompatible materials can be obtained. Thin-film hybrids of calcium phosphate with thicknesses on the submicrometer scale were previously reported to have been obtained through biomimetic methods.[4] However, free-standing films with ordered nanocrystalline hydroxyapatite of several hundred nanometers have not yet been obtained. Our strategy here is to fabricate HAP-based thin-film hybrids with ordered structures through a self-organization process inspired by biomineralization.

Preparation of ordered hybrids of calcium phosphate crystals is desirable for the development of structural and functional hybrid materials.[5,6] HAP-based hybrids are also candidates for biomedical materials such as drug delivery systems and scaffolds applicable to the regeneration of hard tissues.[7] In particular, thin films and coating materials based on calcium phosphate crystals are utilized to control interactions between artificial hard materials and natural hard tissues. Kokubo and coworkers proposed a biomimetic process for coating a layer of HAP similar to bone minerals using simulated body fluid (SBF) and its modified solutions.[8] Processes were also developed to prepare a bone-like HAP layer on various organic substrates.[9]

In our previous work, we have successfully developed not only thin films[2c,d,10,11] but also free-standing thin-film hybrids[12] of $CaCO_3$ and $SrCO_3$ by mimicking the structure of nacre of seashells. Cooperative interactions between soluble acidic polymer additives such as poly(acrylic acid) (PAA) and

[a] *Department of Chemistry and Biotechnology, School of Engineering, The University of Tokyo, Hongo, Bunkyo-ku, Tokyo 113-8656, Japan. E-mail: kato@chiral.t.u-tokyo.ac.jp*
[b] *Department of Crystalline Materials Science, Graduate School of Engineering, Nagoya University, Furo-cho, Chikusa-ku, Nagoya 464-8603, Japan*
† Electronic supplementary information (ESI) available. See DOI: 10.1039/c6ce01336h
‡ Present address: Division of Material Sciences, Kanazawa University, Kakuma-machi, Kanazawa 920-1192, Japan.

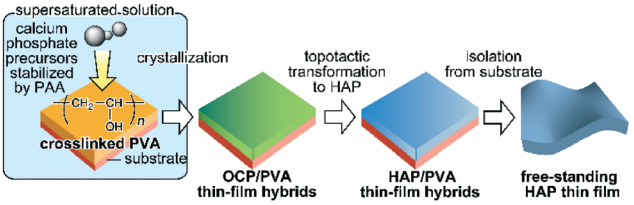

Fig. 1 Schematic illustration of the approach in the present study: development of a free-standing HAP-based thin film.

insoluble organic matrices such as poly(vinyl alcohol) (PVA) play key roles in the formation of thin-film hybrids.[13] PVA has a high density of hydroxyl groups, which are compatible with aqueous ionic solutions.[10b,c] Moreover, the crystal growth and polymorphism of the crystals in the polymer matrices were found to be tuned by the density of crosslinking.[10d] Our approach is to use these cooperative interactions for the preparation of HAP-based thin-film hybrids. Recently, free-standing thin films based on HAP were reported by Imai[14] and Wang.[15] In these cases, films with 10–20 μm thickness were obtained by a solution–air interface process. Jensen *et al.* prepared transparent HAP aggregates on the millimetre scale by sedimentation of HAP nanocrystals.[16] Our intension is to prepare HAP-based free-standing thin films with a thickness of less than 1 μm for versatile applications.

We herein report on a novel approach to the fabrication of thin-film HAP/PVA nanohybrids (Fig. 1). To achieve synthesis of HAP-based nanohybrids with submicrometer thickness, we have developed a process of transforming octacalcium phosphate (OCP; $Ca_8H_2(PO_4)_6{\cdot}5H_2O$) crystals to HAP nanorods.

Experimental section

Materials

Poly(vinyl alcohol) (PVA) (Mw: 1.46×10^5–1.86×10^5; 87–89% hydrolyzed) and poly(acrylic acid) (PAA) (Mw: 2.0×10^3) were purchased from Sigma-Aldrich. Calcium chloride ($CaCl_2$, >95.0%), dipotassium hydrogen phosphate (K_2HPO_4, >99.0%) and dimethyl sulfoxide (DMSO, >99.0%) were obtained from Wako. All chemical compounds were used without further purification. The water used in this study was produced by an Autopure WT100 system (Yamato, Tokyo) and had a relative resistivity of about 1.8×10^7 Ω cm.

Preparation of hybrid thin films

PVA matrices were obtained by a method reported previously.[10d,f] 4 wt% PVA in DMSO solution was spin-coated on glass substrates (30 mm × 30 mm) at 1500 rpm for 60 s. A water-insoluble PVA matrix was obtained after annealing at 200 °C for 60 min. The resultant PVA matrix on a glass substrate was placed at the bottom of a plastic vessel. Then, 2.5 ml of a $CaCl_2$ aqueous solution containing dissolved PAA and an equal amount of a K_2HPO_4 (Wako) aqueous solution was poured into the vessel. The final concentration of $CaCl_2$, K_2HPO_4, and PAA in the crystallization solution was adjusted to 20 mM, 20 mM, and 7.2×10^{-2} wt%, respectively. The polymer matrices were soaked in the crystallization solution for 7 days at room temperature to allow the complete crystallization in the PVA matrix. The sample was washed with purified water and dried in air. Transformation of the hybrids was conducted in water. An appropriate amount of water was poured into a Petri dish. The thin-film hybrids on a glass substrate were soaked in hot water at 80 °C for 60 min. They were washed with purified water and dried at room temperature.

Characterization of the hybrids

The morphologies of the resultant thin-film hybrids were observed using a polarizing optical microscope (POM) (OLYMPUS, BX51), a scanning electron microscope (SEM) (Hitachi, S-4700, operated at 3.0 kV) and a transmission electron microscope (TEM) (JEOL, JEM-2010HC, operated at 200 kV). SEM observations of the samples were performed after platinum coating using a Hitachi E-1030 ion-sputterer, and no conductive treatments were performed during the TEM observation. X-ray diffraction (XRD) (Rigaku, SmartLab) patterns were obtained by a paralleling method with Cu Kα radiation (λ = 0.154 nm) using 2θ and $2\theta\chi$ scanning methods for out-of-plane and in-plane measurements, respectively. To examine the crystallographic orientation, XRD measurements were conducted in in-plane and out-of-plane geometries, wherein the scanning direction is parallel to the substrate and non-parallel to the substrate, respectively. The composition of the crystals formed in the PVA matrix was determined using an inductively-coupled plasma atomic emission spectrometer (ICP/AES) (Thermo Scientific, iCAP DUO-6300). Thermogravimetric (TG) (Rigaku, TG-8120) measurements were conducted under a flow of N_2 (100 cm^3 min^{-1}) up to 1000 °C at a heating rate of 5 °C min^{-1}.

Results and discussion

PVA was used as a matrix of crystallization of calcium phosphate to form HAP-based nanohybrids. PVA matrices were obtained by spin coating of a DMSO solution of PVA onto glass substrates. The matrices were then annealed.[10d,f] For the preparation of precursor thin films of calcium phosphate, the insoluble PVA matrices were soaked in a crystallization solution containing $CaCl_2$, K_2HPO_4, and PAA for 7 days at room temperature. The initial pH of the crystallization solution was 6.2. Subsequently, the precursor hybrid thin films were soaked into 80 °C water for 1 hour to obtain HAP/polymer hybrid thin films.

Thin-film crystals were successfully formed on the PVA matrices after 7 days (Fig. 2a). The X-ray diffraction (XRD) measurements of the thin-film crystals were conducted in out-of-plane and in-plane geometries to characterize the crystal structures (Fig. 2b). These two patterns of the hybrid are ascribed to the characteristic peaks of OCP (ICDD: no. 26-1056). The two peaks observed in the in-plane XRD pattern at 26° and 53° are attributable to the 002 and 004 reflections of

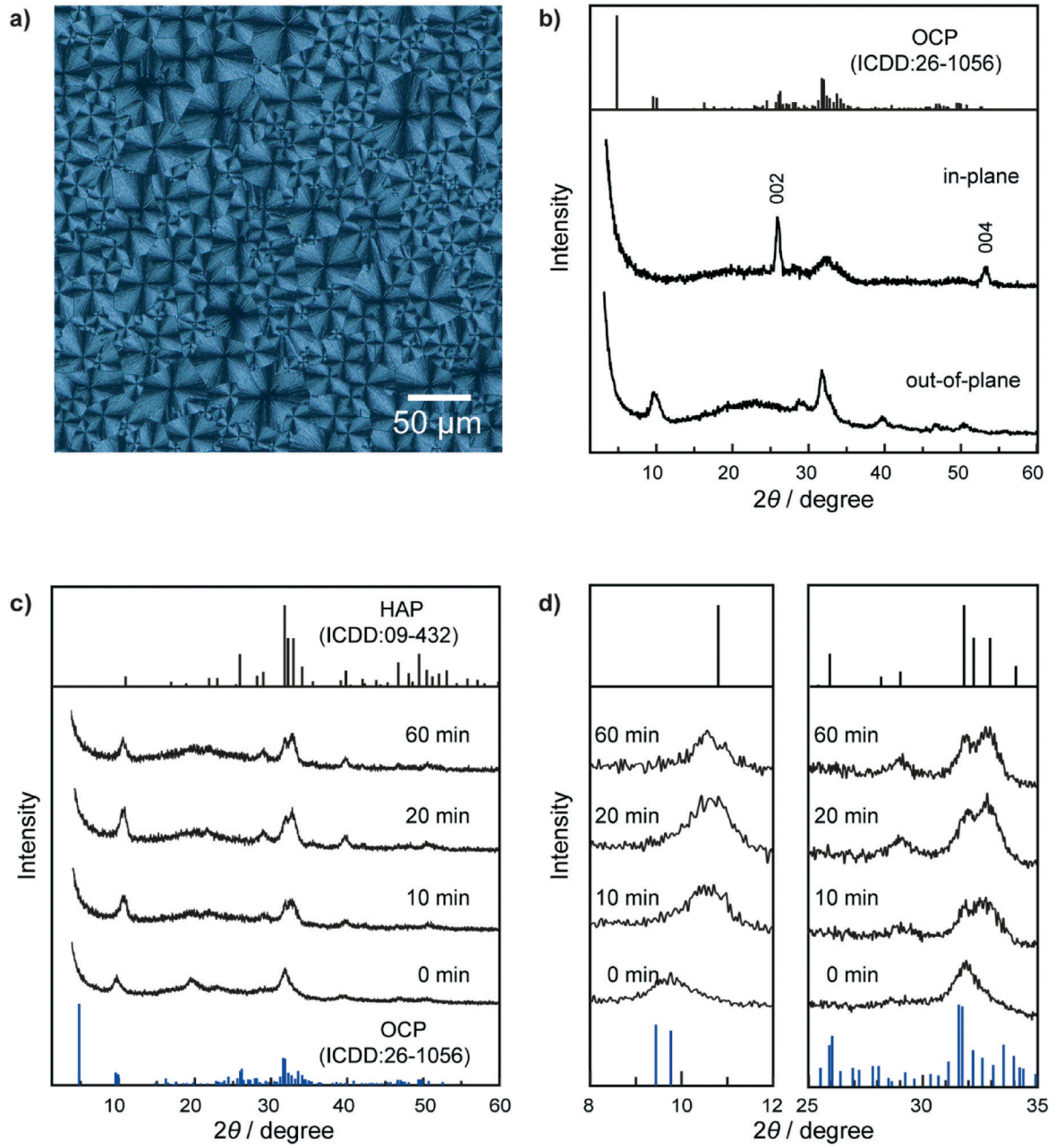

Fig. 2 (a) Polarizing optical micrograph of the thin-film OCP/PVA hybrids. (b) In-plane and out-of-plane XRD patterns of the thin-film OCP/PVA hybrids measured at 0.1° min^{-1}. The upper trace shows the standard powder diffraction pattern of OCP crystals obtained from ICDD (no. 26-1056). (c) XRD patterns of the original OCP/PVA hybrids and the HAP/PVA hybrids obtained by soaking in water at 80 °C for 10, 20, and 60 minutes. The scanning rate for the XRD measurements is 1° min^{-1}. (d) Enlarged patterns of the samples in the angular regions from 8° to 12° (left) and from 25° to 35° (right). The standard powder XRD patterns of OCP and HAP are listed in ICDD (OCP: no. 26-1056, HAP: no. 09-432).

OCP, respectively. Compositional analysis of the thin-film crystals formed on the matrix was performed using inductively-coupled plasma atomic emission spectroscopy (ICP/AES). The molar ratio of calcium to phosphorus (Ca/P) in the resultant hybrids was determined to be 1.49. This value is larger than the stoichiometric composition of OCP (1.33). The larger Ca/P ratio of the resultant thin-film hybrids is attributable to a defective structure in OCP crystals. The defective structure may cause broadening of the peaks, as observed in the XRD pattern (Fig. 2b). Disappearance of the 010 reflection at 4.7°, which is the characteristic peak of OCP, may be attributed to the small crystallite size of the crystals. In addition, the Ca/P ratio 1.49 is ascribed to the existing calcium ions included in the organic matrices consisting of PVA and PAA.

Observation of the hybrids using a polarizing optical microscope reveals that the hybrids are assemblies of spherulitic crystals 10–50 μm in domain size (Fig. 2a). Although the

hybrids are composed of OCP with defective structures, birefringence of the hybrids is clearly observed as a cross-extinction pattern under a polarizing optical microscope (POM). The cross-extinction pattern suggests that the thin-film crystals formed on the PVA matrix exhibit self-assembled structures with aligned optical axes of the OCP crystals in the radial direction of spherulitic thin films. In the XRD measurements, the 00*l* reflections appear only in the in-plane XRD pattern (Fig. 2b). The resultant thin-film hybrids based on the OCP crystals form oriented structures with their *c* axes parallel to the substrates. The hybrids consisting of PVA and OCP with the self-assembled structures were successfully converted to HAP/PVA hybrids in water at 80 °C. The transformation from OCP to HAP was confirmed by the change in their XRD patterns, as shown in Fig. 2c. The peak at 10.8° attributed to the 100 reflection of HAP is observed in the XRD pattern (Fig. 2d, left) of the samples soaked in water at 80 °C for 10 min, while the OCP peak at 9.5° disappears in the XRD pattern (Fig. 2d, left) of the hybrids after 20 min of reaction. The broad peak around 32° due to the OCP crystals is shifted and results in the peak around 33° attributed to the 112, 211, and 300 reflections of HAP (Fig. 2d, right). All the peaks observed in the XRD patterns of the sample after 20 min of reaction can be assigned to the HAP phase. The XRD pattern of the sample after 60 min of reaction is almost the same as that of the sample after 20 min of reaction. The birefringence of the thin-film hybrids disappears as the sample was transformed into HAP (Fig. S1†). Dark images are observed under cross-polarization after soaking in hot water for 20 min, suggesting the completion of transformation (Fig. S1†). The measured value of the Ca/P molar ratio in the transformed materials by ICP/AES suggests that the HAP/PVA hybrids had a larger Ca/P ratio (1.70) compared to the value of the stoichiometric composition of HAP (1.67), after 60 min of reaction. This value of the Ca/P ratio being larger than the stoichiometric value suggests that HAP has nonstoichiometric compositions due to a defective structure and substitution of phosphate ions in the crystals, as well as the Ca^{2+} ion included in the organic polymers existing in the samples after the treatment for the transformation of OCP to HAP in the hybrids. The transformation into HAP in water at 80 °C was also confirmed by means of the FTIR spectra (Fig. S2†).

Macroscopic crystallographic orientation within the HAP-based hybrids, after soaking in hot water for 60 min, was confirmed by XRD measurements (Fig. 3). The *hk*0 reflections are observed as intense peaks in the out-of-plane XRD pattern of the thin-film HAP-based hybrids compared with the standard powder diffraction (Fig. 3). Besides, the 00*l* reflections of HAP crystals appeared only in the in-plane XRD pattern, which is comparable with the OCP/PVA thin-film hybrids (Fig. 2c,d and 3). It should be noted that these XRD measurements suggest that the macroscopic orientation of the *c* axes in the hybrids is preserved through the transformation in hot water.

Fig. 4 shows the hybrid thin films of calcium phosphates before and after the conversion. Macroscopic POM

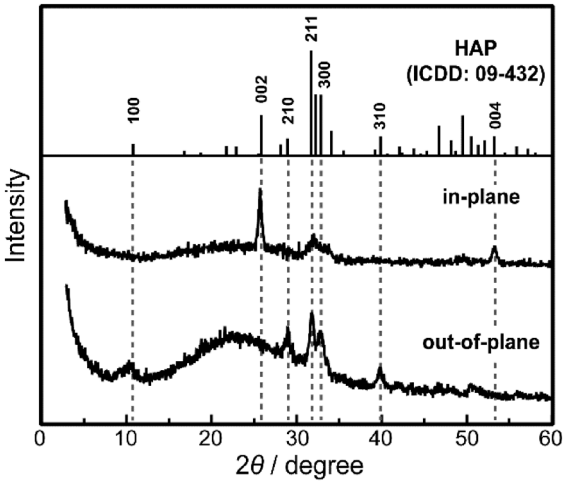

Fig. 3 In-plane and out-of-plane XRD patterns of the HAP/PVA hybrids measured at the scanning rate of 0.1° min^{-1}. The upper trace shows the standard powder XRD pattern of HAP crystals from ICDD (no. 09-432).

and SEM images of the OCP/PVA hybrid thin films (Fig. 4a and b) show assembled structures of spherulitic thin-film crystals 10–50 μm in domain size. The thickness of the thin-film OCP/PVA hybrids is estimated to be 800 nm based on the cross-sectional SEM image (Fig. 4c). HAP/PVA hybrids prepared from precursor OCP/PVA hybrids also exhibit domain structures 10–50 μm in diameter (Fig. 4e and f). The thickness of the hybrids decreased from 800 to 400 nm on transformation (Fig. 4g). In both fractured surfaces of OCP/PVA and HAP/PVA hybrids, no boundaries between the inorganic crystals and the PVA matrices are observed. This biomineralization-inspired crystallization of calcium phosphates develops hybrid structures comprising OCP nanocrystallites and PVA matrices (Fig. 4d). These hybrid structures are maintained until the transformation into HAP hybrids (Fig. 4h).

The size and morphology of the nanocrystallites formed in the PVA matrices are observed using transmission electron microscopy (TEM) (Fig. 5). Fig. 5a shows that assemblies of OCP nanocrystals are formed in the PVA matrix. The corresponding selected-area electron diffraction (SAED) pattern shown in Fig. 5b suggests that the OCP crystals in the assembled structures are oriented in the *c*-axis direction. The TEM image of the HAP/PVA hybrids shows oriented nanorods 4–6 nm in width and 20–50 nm in length (Fig. 5c). The direction of the *c*-axis of HAP corresponds to the long axis of the nanorods, which is confirmed by the localized 002 reflection in the SAED pattern similar to that of the OCP assemblies (Fig. 5d). It is considered that the OCP nanocrystallites formed in the PVA matrix exhibit rod-like morphologies with elongated *c* axes. The size of the OCP nanocrystallites is estimated to be 3 nm in width and 20–30 nm in length, based on Fig. 5a. The size of the nanocrystallites may cause the disappearance of the characteristic peak assigned to the 010 reflection (d = 18.7 Å) of OCP in the XRD pattern (Fig. 2b).

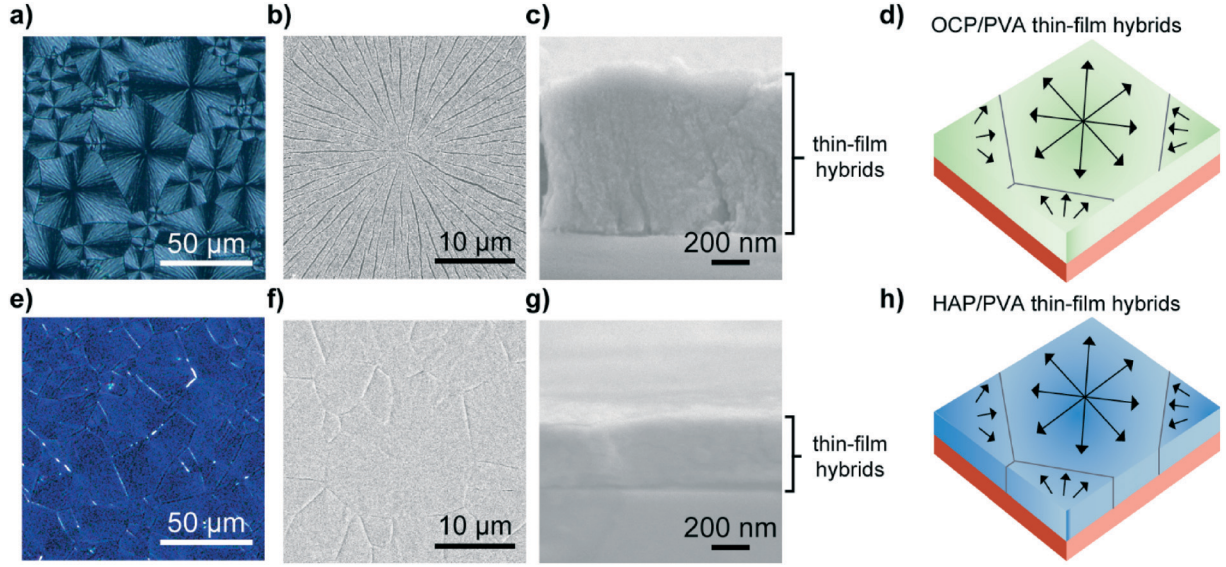

Fig. 4 OCP/PVA thin-film hybrids (a–d) and HAP/PVA thin-film hybrids (e–h) prepared from the OCP/PVA thin-film hybrids. These hybrids are formed on glass substrates. Polarizing optical micrographs (a and e) and SEM images of top-view surfaces (b and f) and fractured surfaces (c and g). (d and h) Schematic illustrations of OCP/PVA and HAP/PVA thin-film hybrids with self-assembled structures. The arrows in (d and h) indicate the direction of crystal growth.

Similar phenomena were observed in exfoliated nanosheet systems of layered inorganic compounds.[17]

It was reported that OCP-like nanocrystals simultaneously transform into HAP crystals accompanied by the release of protons because the OCP-like phase is an intermediate phase.[18] However, in the present case, the polymer matrices and the relatively low pH condition inhibit the simultaneous transformation into HAP crystals within a week, resulting in the formation of intermediate OCP nanocrystals in the PVA matrices.

The transformation into HAP from the intermediate OCP phase can be induced by the hydrothermal process. It should be noted that the OCP crystals can be topotactically transformed into HAP crystals because of similarities in their crystal structures.[19] The rod-like morphologies and oriented structures in the HAP-based hybrids should be adapted from original OCP nanorod crystallites in the hybrids.

It is significant that the transformation from OCP/PVA to HAP/PVA proceeded rapidly, compared with other studies conducted in water, below the boiling point.[20] The OCP crystals in the hybrids were completely transformed into HAP crystals within 20 min. The nanocrystallites with a larger surface area contribute to the rapid transformation, as well as the defective structure of the intermediate OCP crystals.

These OCP/PVA and HAP/PVA hybrids were isolated from the glass substrates as freestanding thin-film hybrids (Fig. 6a and b). These free-standing thin films exhibited colors that can be ascribed to their submicrometer thickness. To evaluate the components of these thin-film hybrids, thermogravimetric (TG) measurements were conducted (Fig. 6c). The TG curves of these thin-film hybrids show weight loss attributable to the water molecules included in the PVA hydrogel below 200 °C and thermal decomposition of the PVA matrix above 200–600 °C (Fig. 6c). Table 1 shows the composition of the OCP/PVA and HAP/PVA hybrids as determined by TG analysis. Due to hydrolysis reaction and dissolution of some inorganic crystals, the amount of inorganic components in the hybrids decreases after the transformation. Consequently, we obtained HAP/PVA hybrids with oriented nanorod structures, with a composition of 6.2 wt% adsorbed water molecules, 42.7 wt% organic polymer and

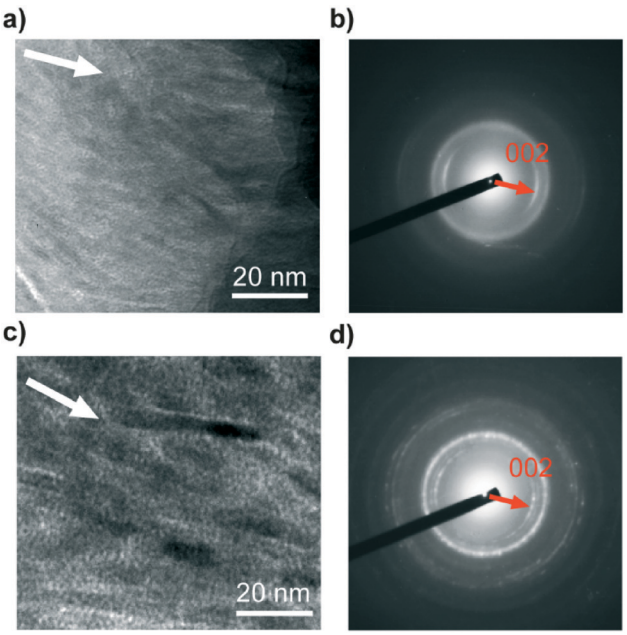

Fig. 5 TEM images and corresponding SAED patterns of the hybrids isolated from glass substrates: OCP/PVA hybrids (a and b) and HAP/PVA hybrids (c and d). The arrows in the TEM images indicate the orientation of the *c* axes of nanocrystallites.

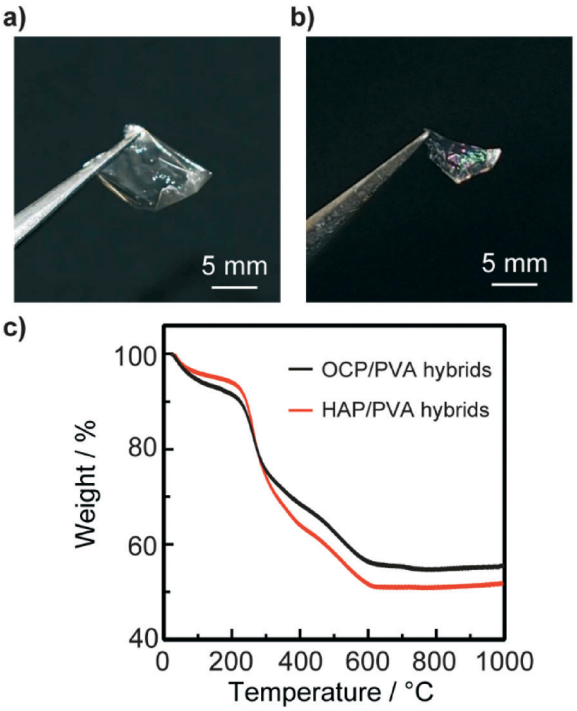

Fig. 6 Photographs of free-standing thin-film OCP/PVA (a) and HAP/PVA (b) hybrids isolated from the glass substrate. The thickness of the isolated thin-film hybrids is several hundred nanometers, estimated from the SEM images shown in Fig. 3. (c) Thermal decomposition behaviors of thin-film OCP/PVA (blue line) and HAP/PVA (black line) hybrids under a N_2 atmosphere.

Table 1 Composition of OCP/PVA and HAP/PVA hybrids as determined by TG analysis

	Adsorbed water molecules	Organic polymers	Inorganic crystals
OCP/PVA hybrids	4.9 wt%	33.7 wt%	61.4 wt%
HAP/PVA hybrids	6.2 wt%	42.7 wt%	51.1 wt%

51.1 wt% inorganic crystal. The HAP/PVA hybrids are similar in structure and composition to bones of vertebrates.[1b]

Conclusions

In summary, we have developed self-standing HAP/PVA thin-film hybrids of submicron thickness. Biomineralization-inspired crystallization under mild conditions led to the formation of oriented nanostructures of OCP/PVA hybrids, which, when soaked in water at 80 °C enable the rapid and topotactic transformation into HAP/PVA hybrids. During the transformation, PVA served as a template to maintain the hybrid structures, resulting in the formation of HAP/PVA thin-film hybrids with oriented nanostructures. It is expected that the thin-film hybrids shall adhere to hard tissues during this conversion. Their free-standing structures and resorbability under physiological conditions should be convenient for tissue engineering in the repair of bones and teeth. Moreover, their structures, composed of oriented nanorod crystals and polymer matrices, are similar to that of the bones of vertebrates. Further biological research is needed to use these hybrids as clinical materials. Moreover, the methods of crystallization described in this study can be utilized for the fabrication of additional inorganic/organic hybrids, which will be candidates for the next generation of environmentally friendly or less-energy-consuming materials.

Acknowledgements

This study was partially supported by KAKENHI JP 22107003 (MEXT) and JP 15H02179 (JSPS). Partial financial support of CREST, JST is also acknowledged. The authors would also like to thank Nanotechnology Platform from The University of Tokyo for the TEM observation.

Notes and references

1 (*a*) *Handbook of Biomineralization*, ed. E. Bäuerlein, P. Behrens and M. Epple, Wiley-VCH, Weinheim, 2007; (*b*) S. Mann, *Biomineralization: Principles and Concepts in Bioinorganic Materials Chemistry*, Oxford University Press, Oxford, 2001; (*c*) W. L. Noorduin, A. Grinthal, L. Mahadevan and J. Aizenberg, *Science*, 2013, **340**, 832–837; (*d*) J. Aizenberg, *MRS Bull.*, 2010, **35**, 323–330; (*e*) F. C. Meldrum and H. Cölfen, *Chem. Rev.*, 2008, **108**, 4332–4432; (*f*) F. Nudelman and N. A. J. M. Sommerdijk, *Angew. Chem., Int. Ed.*, 2012, **51**, 6582–6596; (*g*) J. C. Weaver, G. W. Milliron, A. Miserez, K. Evans-Lutterodt, S. Herrera, I. Gallana, W. J. Mershon, B. Swanson, P. Zavattieri, E. DiMasi and D. Kisailus, *Science*, 2012, **336**, 1275–1280; (*h*) T. Kato, A. Sugawara and N. Hosoda, *Adv. Mater.*, 2002, **14**, 869–877; (*i*) A. Arakaki, K. Shimizu, M. Oda, T. Sakamoto, T. Nishimura and T. Kato, *Org. Biomol. Chem.*, 2015, **13**, 974–989; (*j*) M. Suzuki, K. Saruwatari, T. Kogure, Y. Yamamoto, T. Nishimura, T. Kato and H. Nagasawa, *Science*, 2009, **325**, 1388–1390; (*k*) S. I. Stupp and P. V. Braun, *Science*, 1997, **277**, 1242–1248; (*l*) S. Weiner and L. Addadi, *J. Mater. Chem.*, 1997, **7**, 689–702; (*m*) H.-B. Yao, H.-Y. Fang, X.-H. Wang and S.-H. Yu, *Chem. Soc. Rev.*, 2011, **40**, 3764–3785; (*n*) M. Nakayama, S. Kajiyama, T. Nishimura and T. Kato, *Chem. Sci.*, 2015, **6**, 6230–6234; (*o*) T. Tajima, A. Tsutsui, T. Fujii, J. Takada and Y. Takaguchi, *Polym. J.*, 2012, **44**, 620–624.

2 (*a*) Y. U. T. Gong, C. E. Killian, I. C. Olson, N. P. Appathurai, A. L. Amasino, M. C. Martin, L. J. Holt, F. H. Wilt and P. U. P. A. Gilbert, *Proc. Natl. Acad. Sci. U. S. A.*, 2012, **109**, 6088–6093; (*b*) H. Imai and Y. Oaki, *MRS Bull.*, 2010, **35**, 138–144; (*c*) A. Sugawara, T. Ishii and T. Kato, *Angew. Chem., Int. Ed.*, 2003, **42**, 5299–5303; (*d*) T. Sakamoto, Y. Nishimura, T. Nishimura and T. Kato, *Angew. Chem., Int. Ed.*, 2011, **50**, 5856–5859.

3 (*a*) S. Weiner and H. D. Wagner, *Annu. Rev. Mater. Sci.*, 1998, **28**, 271–298; (*b*) L. C. Palmer, C. J. Newcomb, S. R. Kaltz, E. D. Spoerke and S. I. Stupp, *Chem. Rev.*, 2008, **108**, 4754–4783.

4 T. Nishimura, H. Imai, Y. Oaki, T. Sakamoto and T. Kato, *Chem. Lett.*, 2011, **40**, 458–460.

5 (*a*) S. I. Stupp and G. W. Ciegler, *J. Biomed. Mater. Res.*, 1992, **26**, 169–183; (*b*) S. I. Stupp, G. C. Mejicano and J. A. Hanson, *J. Biomed. Mater. Res.*, 1993, **27**, 289–299; (*c*) S. I. Stupp, J. A. Hanson, J. A. Eurell, G. W. Ciegler and A. Johnson, *J. Biomed. Mater. Res.*, 1993, **27**, 301–311; (*d*) T. Kawai, C. Ohtsuki, M. Kamitakahara, T. Miyazaki, M. Tanihara, Y. Sakaguchi and S. Konagaya, *Biomaterials*, 2004, **25**, 4529–4534; (*e*) C. J. Newcomb, R. Bitton, Y. S. Velichko, M. L. Snead and S. I. Stupp, *Small*, 2012, **8**, 2195–2202; (*f*) T. Taguchi, A. Kishida and M. Akashi, *Chem. Lett.*, 1998, **27**, 711–712; (*g*) N. J. Shah, J. Hong, M. N. Hyder and P. T. Hammond, *Adv. Mater.*, 2012, **24**, 1445–1450; (*h*) J.-J. Guan, B. Tian, S. Tang, Q.-F. Ke, C.-Q. Zhang, Z.-A. Zhu and Y.-P. Guo, *J. Mater. Chem. B*, 2015, **3**, 1655–1666.

6 (*a*) R. Murugan and S. Ramakrishna, *Compos. Sci. Technol.*, 2005, **65**, 2385–2406; (*b*) S. S. Jee, R. K. Kasinath, E. DiMasi, Y. Y. Kim and L. Gower, *CrystEngComm*, 2011, **13**, 2077–2083; (*c*) J. Fletcher, D. Walsh, C. E. Fowler and S. Mann, *CrystEngComm*, 2011, **13**, 3692–3697; (*d*) F. Nudelman, K. Pieterse, A. George, P. H. H. Bomans, H. Friedrich, L. J. Brylka, P. A. J. Hilbers, G. de With and N. A. J. M. Sommerdijk, *Nat. Mater.*, 2010, **9**, 1004–1009; (*e*) A. Dey, P. H. H. H. Bomans, F. A. Muller, J. Will, P. M. Frederik, G. de With and N. A. J. M. Sommerdijk, *Nat. Mater.*, 2010, **9**, 1010–1014; (*f*) Y. Y. Hu, X. P. Liu, X. Ma, A. Rawal, T. Prozorov, M. Akinc, S. K. Mallapragada and K. Schmidt-Rohr, *Chem. Mater.*, 2011, **23**, 2481–2490; (*g*) C. Li, A. Born, T. Schweizer, M. Zenobi-Wong, M. Cerruti and R. Mezzenga, *Adv. Mater.*, 2014, **26**, 3207–3212; (*h*) Y. Takeoka, M. Hayashi, N. Sugiyama, M. Yoshizawa-Fujita, M. Aizawa and M. Rikukawa, *Polym. J.*, 2015, **47**, 164–170; (*i*) W.-X. He, A. K. Rajasekharan, A. R. Tehrani-Bagha and M. Andersson, *Adv. Mater.*, 2015, **27**, 2260–2264; (*j*) K. Iijima, H. Nagahama, A. Takada, T. Sawada, T. Serizawa and M. Hashizume, *J. Mater. Chem. B*, 2016, **4**, 3651–3659.

7 (*a*) M. Antonietti, M. Breulmann, C. G. Göltner, H. Cölfen, K. K. W. Wong, D. Walsh and S. Mann, *Chem. – Eur. J.*, 1998, **4**, 2493–2500; (*b*) K. K. Perkin, J. L. Turner, K. L. Wooley and S. Mann, *Nano Lett.*, 2005, **5**, 1457–1461; (*c*) A. Sugawara, S. Yamane and K. Akiyoshi, *Macromol. Rapid Commun.*, 2006, **27**, 441–446; (*d*) S. Yamane, A. Sugawara, Y. Sasaki and K. Akiyoshi, *Bull. Chem. Soc. Jpn.*, 2009, **82**, 416–418; (*e*) M. Z. Zhang, A. Ishii, N. Nishiyama, S. Matsumoto, T. Ishii, Y. Yamasaki and K. Kataoka, *Adv. Mater.*, 2009, **21**, 3520–3525; (*f*) S. P. Pathi, D. D. W. Lin, J. R. Dorvee, L. A. Estroff and C. Fischbach, *Biomaterials*, 2011, **32**, 5112–5122; (*g*) H. Imai, S. Tatara, K. Furuichi and Y. Oaki, *Chem. Commun.*, 2003, 1952–1953; (*h*) J. Song, E. Saiz and C. R. Bertozzi, *J. Am. Chem. Soc.*, 2003, **125**, 1236–1243; (*i*) L. Li, C. Y. Mao, J. M. Wang, X. R. Xu, H. H. Pan, Y. Deng, X. H. Gu and R. K. Tang, *Adv. Mater.*, 2011, **23**, 4695–4701.

8 (*a*) Y. Abe, T. Kokubo and T. Yamamuro, *J. Mater. Sci.: Mater. Med.*, 1990, **1**, 233–238; (*b*) M. Tanahashi, T. Yao, T. Kokubo, M. Minoda, T. Miyamoto, T. Nakamura and T. Yamamuro, *J. Am. Ceram. Soc.*, 1994, **77**, 2805–2808.

9 (*a*) T. Miyazaki, C. Ohtsuki, Y. Akioka, M. Tanihara, J. Nakao, Y. Sakaguchi and S. Konagaya, *J. Mater. Sci.: Mater. Med.*, 2003, **14**, 569–574; (*b*) A. Oyane, M. Kawashita, K. Nakanishi, T. Kokubo, M. Minoda, T. Miyamoto and T. Nakamura, *Biomaterials*, 2003, **24**, 1729–1735; (*c*) C. Ohtsuki, M. Kamitakahara and T. Miyazaki, *J. Tissue Eng. Regener. Med.*, 2007, **1**, 33–38; (*d*) S. Morimune-Moriya, S. Kondo, A. Sugawara-Narutaki, T. Nishimura, T. Kato and C. Ohtsuki, *Polym. J.*, 2015, **47**, 158–163.

10 (*a*) T. Kato, *Adv. Mater.*, 2000, **12**, 1543–1546; (*b*) F. J. Zhu, T. Nishimura, T. Sakamoto, H. Tomono, H. Nada, Y. Okumura, H. Kikuchi and T. Kato, *Chem. – Asian J.*, 2013, **8**, 3002–3009; (*c*) S. Kajiyama, T. Nishimura, T. Sakamoto and T. Kato, *Small*, 2014, **10**, 1634–1641; (*d*) T. Sakamoto, A. Oichi, T. Nishimura, A. Sugawara and T. Kato, *Polym. J.*, 2009, **41**, 522–523; (*e*) F. J. Zhu, T. Nishimura and T. Kato, *Polym. J.*, 2015, **47**, 122–127; (*f*) T. Sakamoto, A. Oichi, Y. Oaki, T. Nishimura, A. Sugawara and T. Kato, *Cryst. Growth Des.*, 2009, **9**, 622–625.

11 (*a*) T. Nishimura, K. Toyoda, T. Ito, Y. Oaki, Y. Namatame and T. Kato, *Chem. – Asian J.*, 2015, **10**, 2356–2360; (*b*) T. Sakamoto, Y. Nishimura and T. Kato, *CrystEngComm*, 2015, **17**, 6947–6954; (*c*) Y. Han, T. Nishimura and T. Kato, *CrystEngComm*, 2014, **16**, 3540–3547.

12 (*a*) Y. Oaki, S. Kajiyama, T. Nishimura, H. Imai and T. Kato, *Adv. Mater.*, 2008, **20**, 3633–3637; (*b*) T. Saito, Y. Oaki, T. Nishimura, A. Isogai and T. Kato, *Mater. Horiz.*, 2014, **1**, 321–325; (*c*) S. Matsumura, S. Kajiyama, T. Nishimura and T. Kato, *Small*, 2015, **11**, 5127–5133.

13 (*a*) F. F. Amos, D. M. Sharbaugh, D. R. Talham, L. B. Gower, M. Fricke and D. Volkmer, *Langmuir*, 2007, **23**, 1988–1994; (*b*) M. Kijima, Y. Oaki and H. Imai, *Chem. – Eur. J.*, 2011, **17**, 2828–2832; (*c*) B. Cantaert, Y. Y. Kim, H. Ludwig, F. Nudelman, N. A. J. M. Sommerdijk and F. C. Meldrum, *Adv. Funct. Mater.*, 2012, **22**, 907–915; (*d*) T. Nishimura, *Polym. J.*, 2015, **47**, 235–243.

14 K. Aita, Y. Oaki, C. Ohtsuki and H. Imai, *CrystEngComm*, 2015, **17**, 5551–5555.

15 Y. F. Xu, G. B. Ma, X. Y. Wang and M. Wang, *Cryst. Growth Des.*, 2012, **12**, 3362–3368.

16 A. C. S. Jensen, C. J. S. Ibsen, D. Sutherland and H. Birkedal, *Cryst. Growth Des.*, 2014, **14**, 6343–6349.

17 (*a*) P. Joensen, R. F. Frindt and S. R. Morrison, *Mater. Res. Bull.*, 1986, **21**, 457–461; (*b*) T. Sasaki, M. Watanabe, H. Hashizume, H. Yamada and H. Nakazawa, *J. Am. Chem. Soc.*, 1996, **118**, 8329–8335; (*c*) K. Fukuda, K. Akatsuka, Y. Ebina, R. Ma, K. Takada, I. Nakai and T. Sasaki, *ACS Nano*, 2008, **2**, 1689–1695.

18 (*a*) W. J. E. M. Habraken, J. Tao, L. J. Brylka, H. Friedrich, L. Bertinetti, A. S. Schenk, A. Verch, V. Dmitrovic, P. H. H. Bomans, P. M. Frederik, J. Laven, P. van der Schoot, B. Aichmayer, G. de With, J. J. DeYoreo and N. A. J. M. Sommerdijk, *Nat. Commun.*, 2013, **4**, 1507; (*b*) C. J. S. Ibsen, D. Chernyshov and H. Birkedal, *Chem. – Eur. J.*, 2016, **22**, 12347–12357.

19 Y. H. Tseng, C. Y. Mou and J. C. C. Chan, *J. Am. Chem. Soc.*, 2006, **128**, 6909–6918.

20 (*a*) W. E. Brown, J. P. Smith, A. W. Frazier and J. R. Lehr, *Nature*, 1962, **196**, 1050–1055; (*b*) M. Iijima, H. Kamemizu, N. Wakamatsu, T. Goto, Y. Doi and Y. Moriwaki, *J. Cryst. Growth*, 1997, **181**, 70–78; (*c*) N. Ito, M. Kamitakahara, S. Murakami, N. Watanabe and K. Ioku, *J. Ceram. Soc. Jpn.*, 2010, **118**, 762–766; (*d*) Y.-H. Tseng, M. E. Birkbak and H. Birkedal, *Cryst. Growth Des.*, 2013, **13**, 4213–4219.